

## Supported Iron Nanoparticles on Activated Carbon, Polyethylene and Silica for Nitrate Reduction

Misun Cho\*, Ewha Kim, Kyoung-Hee Lee and Samyoung Ahn

*Department of Environmental Education, Suncheon National University, Suncheon, Jeonnam 540-742, Korea*

*\*Department of Chemical Education, Suncheon National University, Suncheon, Jeonnam 540-742, Korea*

(Manuscript received 17 March, 2008; accepted 4 July, 2008)

### Abstract

The use of support materials on the nanoparticle synthesis and applications has advantages in many aspects; resisting the aggregation and gelation of nanoparticles, providing more active sites by dispersing over the supports, and facilitating a filtering process. In order to elucidate the influence of the supports on the nitrate reduction reactivity, the supported iron nanoparticles were prepared by borohydride reduction of an aqueous iron salt in the presence of supports such as activated carbon, silica and polyethylene. The reactivity for nitrate reduction decreased in the order of unsupported Fe(0) > activated carbon(AC) supported Fe(0) > polyethylene(PE) supported Fe(0)  $\geq$  silica supported Fe(0). Rate constants decrease with increasing initial nitrate concentration implying that the reaction is limited by the surface reaction kinetics.

**Key Words :** Supported iron nanoparticles, Nitrate reduction, Activated carbon, Polyethylene, Silica

### 1. Introduction

Due to the recent development of nanotechnology, researchers in environmental science have also shown interest in nano-sized agents to improve the efficiency of chemical treatment to control contaminants. Nano-sized zerovalent iron has shown an improved reactivity compared to micro- or milli-sized iron for the dechlorination of halogenated organic contaminants<sup>1,2</sup>, reduction of Cr(VI) and Pb(II) to Cr(III) and Pb(0)<sup>3</sup>, and nitrate reduction<sup>4</sup>. While the small size of nanoparticles and therefore greatly increased specific surface area are advantageous in the context of reactivity improvement, it is often detrimental in other respects. Due to the small size and colloidal character, the separation of nanoparticles from the reaction solution is an expensive process. Clumping of nanoparticles in col-

umn would adversely affect permeability and would impede the flow of water through it. Adhesion of nanoparticles on larger support particles could overcome this problem. Nano size particles can be tethered on to larger supports for greater ease of separation and for improvement of hydraulic conductivity. In addition, dispersion of the active metals in nanoscale on the support material with large surface area can offer a large number of active sites.

Supports have been widely used to prepare heterogeneous catalysts in many industries, such as chemical, petrochemical and pharmaceutical sectors. These supports are required to provide a sound base on which to disperse the active catalyst component and stabilize the catalyst phase, and withstand the conditions within the chemical reactor<sup>5</sup>. The activity of a supported reagent is strongly related to the chemical composition and characteristics of supporting materials and also morphology, such as size and shape.

Although iron in nitrate reduction is not a catalyst and the role of supports in this study may differ from

---

Corresponding Author : Samyoung Ahn, Address: Department of Environmental Education, Suncheon National University, Choongang-ro, Suncheon, Jeonnam 540-742 Korea  
Phone: +82-61-750-3381  
E-mail: sahn@sunchon.ac.kr

that of catalytic reactions, understanding the chemical and physicochemical features of supports and subsequent changes on the surface environment of an adsorbed reagent is crucial to selecting supports. While there has been an extensive literature on the supported catalysts<sup>5)</sup>, only few reports refer to the supported iron in stoichiometric reactions<sup>3,6)</sup>, and information for the selection of the support for remediation of environmental pollutants is lacking.

The objective of the proposed study is to investigate the influence of the diverse supports on the nitrate reduction by iron nanoparticles and make a comparison of the reactivity between unsupported iron nanoparticles and supported iron nanoparticles. Activated carbon(AC) and silica were chosen as supports because these are porous materials with large surface area and the active metals can disperse in nanoscale forming large amount of active sites. Polyethylene(PE) is a nonporous polymer, however, it can also be used for a similar purpose; resisting aggregation of nanoparticles and dispersing the active metals. Besides, polyethylene is easy to form a certain shape and size, and its low density compared to inorganic supports reduces the weight of treatment equipment.

## 2. Materials and Methods

$\text{FeSO}_4 \cdot 7\text{H}_2\text{O}$  (99+%) was obtained from Kanto Chemical Co.(Japan), and  $\text{KBH}_4$  (98%) was obtained from Aldrich. Activated carbon was purchased from Aldrich (Darco.12-20 mesh) and used after washing with deionized water. Silica was purchased from Merck(silica gel 60) and used as received. Polyethylene was supplied by LG Chemical Co. (Korea). All aqueous solutions were made in water purified with a Milli-Q system ( $18 \text{ M}\Omega \cdot \text{cm}$ ). All procedures for syntheses and handling during this experiment were carried out under an atmosphere of  $\text{N}_2$  (99.9%), using standard Schlenk and vacuum line techniques<sup>7)</sup>. All solvents were degassed and saturated with  $\text{N}_2$  before use.

Based on the literatures<sup>3,8)</sup>, the supported iron nanoparticles were synthesized by adding  $\text{KBH}_4$  solution to  $\text{FeSO}_4 \cdot 7\text{H}_2\text{O}$  solution (mol ratio of  $\text{KBH}_4$ :  $\text{FeSO}_4 \cdot 7\text{H}_2\text{O}$

= 2.5:1) in the presence of a given amount of support materials. We chose the weight ratio of 4:1 for Fe(0): supports, as at the higher ratio of supports the reduction of nitrate did not take place. After addition of the  $\text{KBH}_4$ , the solution was stirred for 15 min. at room temperature. The metal particles formed were settled, the supernatant was decanted with a double-tipped needle. Then the solid was washed with degassed and deionized water several times and finally with degassed acetone. The resulting gray-black solid was vacuum-dried.

For the batch experiment, typically, a given amount of supported iron nano particles was charged into a Schlenk flask containing 350 mL of nitrate solution under stirring. The nitrate solution was deoxygenated by a  $\text{N}_2$  stream for 2 h before adding iron. Periodically, 10 mL samples were withdrawn under a  $\text{N}_2$  stream and filtered through a  $0.45 \mu\text{m}$  membrane filter (Advantec MFS). The concentrations of nitrate and nitrite were determined by ion chromatography (Dionex 120). Samples for the determination of ammonia were treated with a few drops of dilute HCl to trap ammonia as ammonium ion, which were then analyzed by UV spectrophotometer (Shimadzu 1600) using the Indophenol method<sup>9)</sup>.

The BET surface area of the synthesized particles was measured using nitrogen adsorption method at Korea Basic Science Institute with a Surface Area Analyzer (ASAP-2010, micromeritics). Metal contents were analyzed at Korea Basic Science Institute with ICP-AES (Jobin Yvon, 138 Ultrace). XRD measurements were performed with PW 1830 APD System (Panalytical, Netherland) equipped with a graphite monochromator (Cu K radiation,  $\lambda = 1.54056 \text{ \AA}$ ). Surface morphologies of nano particles were examined by a Field Emission Scanning Electron Microscope (FE-SEM, Hitachi S-4700) operating at an acceleration voltage of 10 kV. The microscopic features of the sample were observed by High-Resolution Transmission Electron Microscope (HR-TEM, JEM2100F, JEOL, Japan, FRG-TEM) operating at 200 kV. Sample for TEM measurement were prepared on 200 mesh copper grid coated with carbon. After diluting the samples to an appropriate concentration in ethanol, the solution was soni-

cated for 10 min., and then a copper grid was carefully dipped into the solution and was dried under ambient temperature. The sample preparation for the measurements of XRD, TEM, and SEM was performed under atmospheric conditions without an air protecting equipment. The pH was measured using HANNA instrument 8520.

### 3. Results and Discussion

#### 3.1. Characterization of the supported iron nanoparticles

The supported iron nanoparticles contained 75.9% iron by weight, as determined by ICP-AES. This value is a little lower than the theoretical value of 80%. Morphology of the supported nanoparticles was determined using SEM and TEM images. Fig. 1 shows the TEM and SEM images of activated carbon supported iron nanoparticles. The average particle size mostly ranged from 50 to 200 nm, and particles were arranged in a chain structure. The magnified high resolution TEM in Fig. 1B reveals that the oxide coating surrounds the large metallic cores with ca. 5 nm thickness. This iron oxide coating is responsible for protecting the zerovalent iron inside the particles against further corrosion. The literature abounds with reports dealing with the formation and structure of the oxide shell<sup>4,10,11</sup>. Compared to the unsupported iron nanoparticles, the presence of supports in the ratio used in our experiments seems to have no influence on the size and structure of particles.

X-ray powder diffraction analyses show the typical signal patterns corresponding to the zerovalent iron

(Fig. 2). A sharp peak at  $2\theta = 26.6$  in Fe/AC can be assigned to the peak of the activated carbon, the diffraction peaks for silica were not observed, which is due to the amorphous nature.

As shown in Table 1, the BET surface area of activated carbon and silicagel is much larger than iron nanoparticles itself, which is known to be av.  $8.10 \text{ m}^2/\text{g}^4$ . Therefore, the surface area of supports themselves are dominant factor in determining the BET surface area of supported iron nanoparticles. Nevertheless, it should be noted that the surface area of the sup-

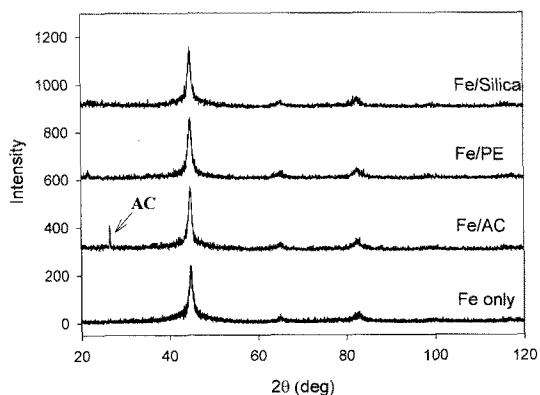


Fig. 2. X-ray powder diffraction patterns of the supported iron nanoparticles.

Table 1. Physical properties of supports

	Activated carbon	Polyethylene	Silicagel
Manufacturer	Aldrich	GS Caltex	Merck
Surface area $\text{m}^2/\text{g}(\text{BET})$	670.53	2.965	480-540
Sieve size(mesh)	12-20	35-50	70-230

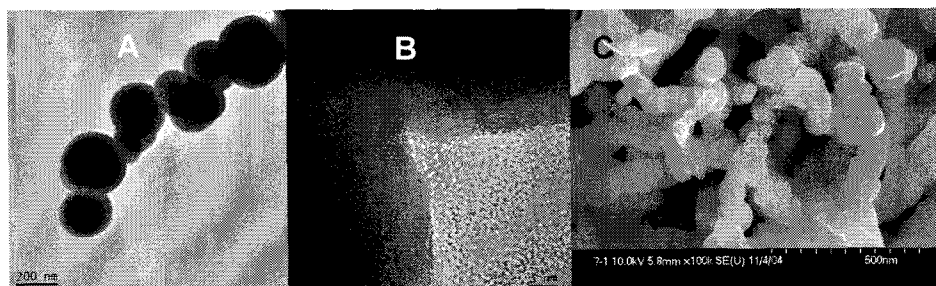


Fig. 1. SEM and TEM images of iron nanoparticles. (A) TEM image (B) HR-TEM image showing iron oxide coating. (C) SEM image.

ported iron nanoparticles decreased significantly upon depositing the iron nanoparticles on those supports. For activated carbon it changed from 670 to 234 m<sup>2</sup>/g, for silica from ca. 510 to 13.4 m<sup>2</sup>/g. Some of the pores of the supports seem to be blocked after loading of iron nanoparticle. Zhu et al.<sup>6</sup> also reported the decrease of the specific surface area of silica supported iron after the loading of iron particles on the silica and reasoned the blockage of silica mesopores. In case of polyethylene(PE) support, the surface area of PE supported iron increased to 10.7 m<sup>2</sup>/g, indicating that the metal particles dispersed in nano size on this non-porous support.

### 3.2. Influence of supports on the reactivity of nitrate reduction

Batch experiments were conducted to compare the reactivity of unsupported iron nanoparticles to those of

the supported iron nanoparticles for nitrate reduction. Kinetic data were calculated from the average values of replicate tests ( $n=3\sim 6$ ) for each set of reactions. Three different iron doses (0.2 g, 0.5 g, and 1 g) with 50 ppm nitrate (50 mg of NO<sub>3</sub><sup>-</sup>/L) in 350 mL solution were tested, and for each iron doses, 20%(w/w) of supports were contained. Nitrate removal rate fits the pseudo-first-order reaction kinetics very well (Fig. 3). The observed rate constants ( $k_{obs}$ ) of the unsupported iron nanoparticles and the supported iron nanoparticles were compared. The rate constants of the unsupported iron nanoparticles are higher than those of the supported iron nanoparticles under the tested experimental conditions. The observed rate constants ( $k_{obs}$ ) of the unsupported iron were 2.26 h<sup>-1</sup> for 0.2 g iron, 5.25 h<sup>-1</sup> for 0.5 g iron, and 10.12 h<sup>-1</sup> for 1 g iron. In case of AC supported iron nanoparticles, the observed rate constants ( $k_{obs}$ ) were 1.40 h<sup>-1</sup> for 0.2 g iron, 2.36 h<sup>-1</sup>

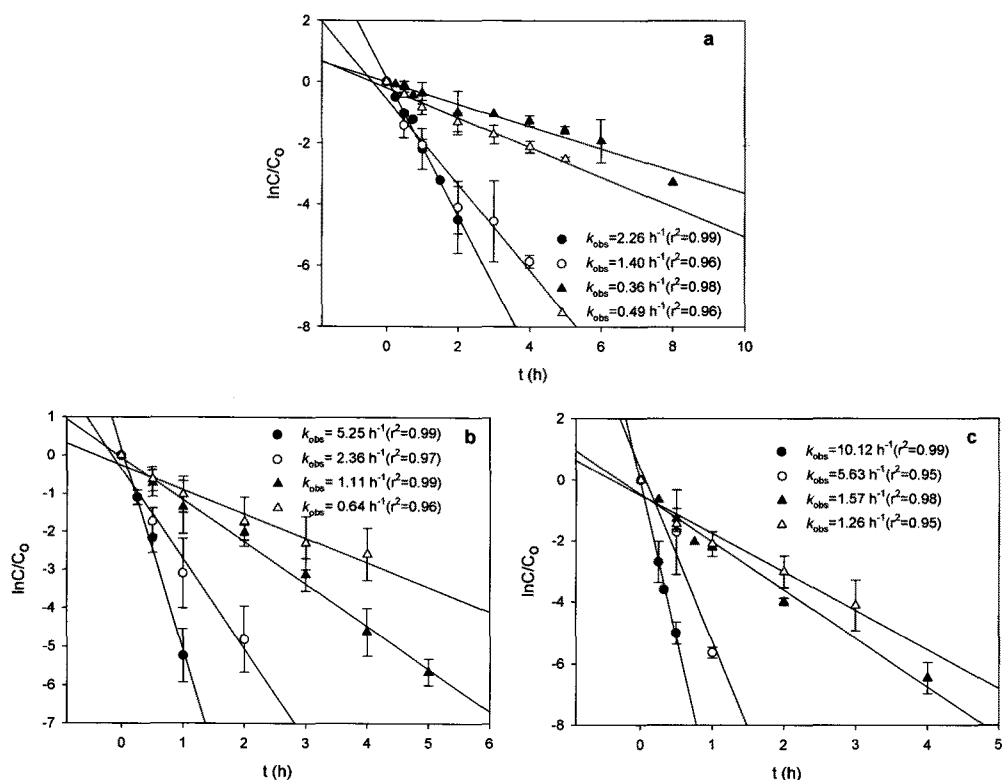


**Fig. 3.** Comparison of rate constants for the nitrate reduction of the unsupported iron nanoparticles and the supported iron nanoparticles (50 ppm nitrate in 350 mL solution). ● unsupported iron, ○ activated carbon supported iron, ▲ polyethylene supported iron, △ silica supported iron. a: 0.2 g iron. b: 0.5 g iron. c: 1 g iron.

for 0.5 g iron, and  $5.63 \text{ h}^{-1}$  for 1 g iron. For PE supported iron, the observed rate constants ( $k_{obs}$ ) were  $0.36 \text{ h}^{-1}$  for 0.2 g iron,  $1.11 \text{ h}^{-1}$  for 0.5 g iron, and  $1.57 \text{ h}^{-1}$  for 1 g iron. The lowest reactivity shows the silica supported iron, so that the observed rate constants ( $k_{obs}$ ) were  $0.49 \text{ h}^{-1}$  for 0.2 g iron,  $0.64 \text{ h}^{-1}$  for 0.5 g iron, and  $1.26 \text{ h}^{-1}$  for 1 g iron.  $R^2$  values ranged from 0.95 to 0.99 in all experiments.

The retarded reactivity of supported iron relative to that of the unsupported iron is due to the physical and chemical changes of environment at the Fe/H<sub>2</sub>O interface, where iron particles reduce nitrate ions.

First, the aforementioned decreased surface area of supported iron nanoparticles, particularly for activated carbon and silica, can be responsible for the decreased reactivity. It is likely that the nucleation of iron nanoparticles takes place inside the pore of a particle to block pores during the nanoparticles synthesis, and so it is difficult for nitrate to reach the inner active metal of porous supports. In addition, even though nitrate is able to reach the iron inside the pore, OH<sup>-</sup>, which is released during the reaction, cannot easily diffuse out and pH-gradient will be built up inside the particles, thereby decreasing the reactivity. It has been reported in many literatures that the increase of pH of solution has a significantly negative impact on the nitrate reduction and the optimum pH should be weakly acidic<sup>4,12-14</sup>.

Second, chemical characteristics of supports can also significantly impact the reactivity. The nitrate reduction by zerovalent iron follows transport-limited kinetics, therefore diffusion-controlled rates can be changed by the chemical and physical feature of diffusion layer at particle surface. Activated carbon is usually categorized as a nonpolar adsorbent to remove the nonpolar or less polar organic compounds in water<sup>15</sup>. The locally nonpolar environments on the activated carbon in aqueous media may repel nitrate ion in the vicinity of iron nanoparticles, it retards the reduction of nitrate by iron.

In the case of polyethylene support, the decreased reaction rate can also be attributed to the nonpolar character of polyethylene. Polyethylene itself is a typical nonpolar organic polymer, therefore it is reluctant to mix with water phase resulting in a hydrophobic

spots on the surface of iron.

Silica particles as a support material impair the reactivity of nitrate reduction in a very different way from activated carbon or polyethylene. Silica in aqueous medium has surface SiOH groups, often denoted  $\equiv\text{Si-O-H}$ , with which zerovalent iron can have an interaction forming  $\equiv\text{Si-OHM}$  and/or  $\equiv\text{Si-OM}^{16}$ . This kind of interaction can induce a positive polarization of electron density of iron resulting in the decline of reactivity of zerovalent iron toward the nitrate reduction.

The influence of iron concentration (0.2 g, 0.5 g, 1 g in 0.35 L) on the rate of nitrate removal is shown in Fig. 4. Increasing the iron loading in the solution increases linearly the reaction rates, regardless of the

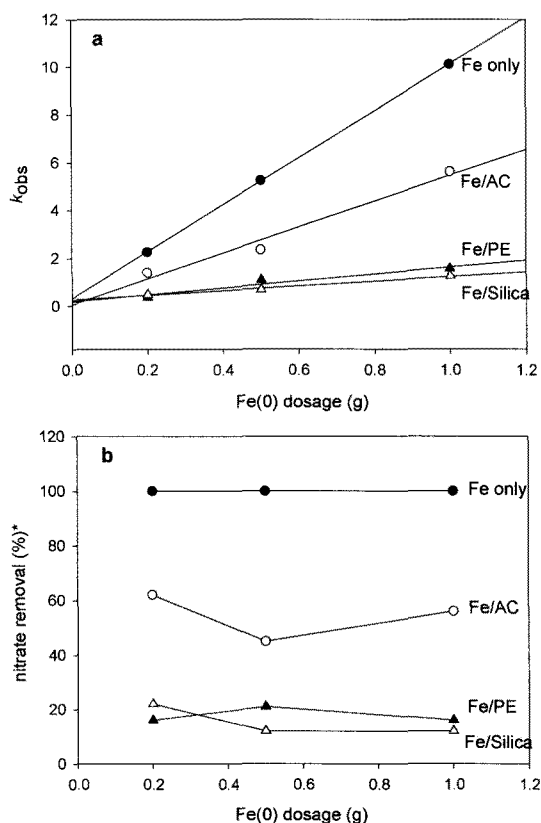
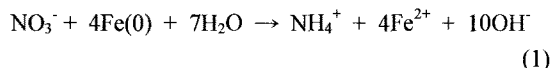


Fig. 4. Effect of iron concentration on reaction rate at the 50 ppm nitrate in 350 mL solution. (a)  $k_{obs}$  vs. iron dosage. (b) Relative nitrate removal of the supported iron. \*The relative removal efficiency of various supported iron is calculated based on the rate constant of unsupported iron.

support types. The reactivity of activated carbon supported iron is ca. 60% of unsupported iron, that of polyethylene and silica are ca. 16% of the unsupported iron, and this tendency is independent on the iron dosage under the experimental condition.

The kinetics of iron mediated reduction reaction is commonly found to follow a Langmuir-Hinshelwood rate expression and the pseudo-first-order rate constants are expected to be invariable according to the initial concentration of reagents. This kinetic model is based on the assumption that the iron exists in large excess in solution. However, Fig. 5 shows a significant dependence of rate constant on initial nitrate concentration. This indicates that substrate coverage on the iron surface was high and there will be competition for active sites, and the reaction is limited by the surface-reaction kinetics<sup>17</sup>.



The overall reaction of zerovalent iron with nitrate is shown in Eq. 1<sup>18</sup>. 0.5 g iron (8.93 mmol) can theoretically reduced 140 mg (2.23 mmol) nitrate, assuming that all of iron is consumed as if reaction runs in homogeneous condition. This iron dose corresponds to 8-times excess for the solution of 50 ppm/350 mL nitrate (0.28 mmol), 4 fold excess for 100 ppm/ 350 mL nitrate, and only 2 fold excess for 200 mg/350 mL nitrate. Considering that such calculation is based on the assumption that the iron particles will be com-

pletely consumed and that in reality, however, only surface iron can participate in the reaction, the amount of available iron is much less than the calculated amount, especially in the higher concentration of nitrate solution. As a result, the active sites available to nitrate ions were insufficient and the interpretation of the experimental result needs an adaptation of the Langmuir-Hinshelwood-Hougen-Watson mode<sup>19</sup>. In this kinetic model, the pseudo-first-order rate constant  $k_{\text{obs}}$  is no longer constant but varies with the concentration of the nitrate. For the supported iron, descent of the reactivity upon a higher nitrate concentration is not so much profound, presumably because of their originally lower reactivity.

Nitrogen mass balance, defined as the percentage of the sum of measured  $\text{NO}_3^-$ ,  $\text{NO}_2^-$ , and  $\text{NH}_4^+$  over initial  $\text{NO}_3^-$ , was in the range of 80–90%, indicating the ammonia is the major end product in the reduction process. A small amount of  $\text{NO}_2^-$  (below 1 ppm) as an intermediate was also detected<sup>4</sup>.

#### 4. Conclusions

The reactivity of unsupported and supported iron nanoparticles for nitrate reduction decreased significantly in the order of unsupported  $\text{Fe}(0)$  > activated carbon supported  $\text{Fe}(0)$  > polyethylene supported  $\text{Fe}(0)$   $\geq$  silica supported  $\text{Fe}(0)$ . These results can be attributed to the decreased specific surface area of supported iron nanoparticles and the alteration of the surface environment of iron onto the supported particles. At higher nitrate concentration, the reduction kinetics seems to follow Langmuir-Hinshelwood-Hougen-Watson model where nitrate molecules compete for a limited number of reactive site on iron surface.

The weight percent of supporting materials to the iron is 25% in all experimental setup, and our result may be restricted to this ratio of support to iron and under this reaction conditions. Nevertheless, this study is the first example to show the influence of supports on iron based chemical treatments of environmental pollutants and it will stimulate subsequent researches not only on the role of the supports in nanoparticle associated reactions, but also on finding a proper support

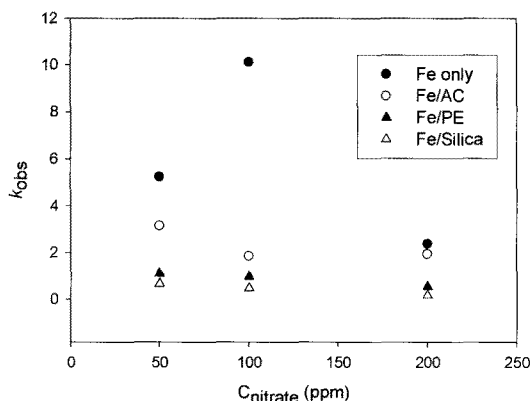


Fig. 5. Effect of nitrate concentration on  $k_{\text{obs}}$  at 0.5 g iron dosage in 350 mL solution.

and reaction conditions to achieve the optimal efficiency of the supported nanoparticle.

### Acknowledgments

This work was supported by the Korea Science & Engineering Foundation (R04-2004-000-10192-0) and 2004 research grant of Sunchon National University.

### References

- 1) Wang C. B., Zhang W. X., 1997, Synthesizing nanoscale iron particles for rapid and complete dechlorination of TCE and PCBs, *Environ. Sci. Technol.*, 31, 2154-2156.
- 2) Li F., Vipulanandan C., Mohanty K. K., 2003, Microemulsion and solution approaches to nanoparticle iron production for degradation of trichloroethylene, *Colloids Surf. A.*, 223, 103-112.
- 3) Ponder S. M., Darab J. G., Mallouk T. E., 2000, Remediation of Cr(VI) and Pb(II) aqueous solutions using supported, nanoscale zero-valent iron, *Environ. Sci. Technol.*, 34, 2564-2569.
- 4) Sohn K., Kang S. W., Ahn S., Woo M., Yang S. K., 2006, Fe(0) nanoparticles for nitrate reduction: stability, reactivity and transformation, *Environ. Sci. Technol.*, 40, 5514-5519.
- 5) Buschow K. H. J., 2001, Supported catalysts, In: *Encyclopedia of materials: Science & Technology*, Elsevier, 9, 8986-8991.
- 6) Zhu B. W., Lim T. T., Feng J., 2006, Reductive dechlorination of 1,2,4-trichlorobenzene with palladized nanoscale Fe<sup>0</sup> particles supported on chitosan and silica, *Chemosphere*, 65, 1137-1145.
- 7) Shriver D. F., Drezdon M. A., 1986, *The manipulation of air-sensitive compounds*, 2nd ed., Wiley, New York.
- 8) Glavee G. N., Klabunde K. J., Sorensen C. M., Hadjipanayis G. C., 1995, Chemistry of borohydride reduction of iron (II) and iron (III) ions in aqueous and nonaqueous media. Formation of nanoscale Fe, FeB, and Fe<sub>2</sub>B powders, *Inorg. Chem.*, 34, 28-35.
- 9) Clesceri L. S., Greenberg A. E., Eaton A. D., 1998, *Standard methods for the examination of water and wastewaters*, 20th ed., American Public Health Association, Washington D.C., 4-108.
- 10) Liu Y., Majetich S. A., Tilton R. D., Sholl D. S., Lowry G. V., 2005, TCE dechlorination rates, pathways, and efficiency of nanoscale iron particles with different properties, *Environ. Sci. Technol.*, 39, 1338-1345.
- 11) Carpenter E. F., Calvin S., Stroud R. M., Harris V. G., 2003, Passivated iron core-shell nanoparticles, *Chem. Mater.*, 15, 3245-3246.
- 12) Alowitz M. J., Scherer M. M., 2002, Kinetics of nitrate, nitrite, and Cr(VI) reduction by iron metal, *Environ. Sci. Technol.*, 36, 299-306.
- 13) Miehr R., Tratnyek M. M., Bandstra J. Z., Scherer M. M., Alowitz M. J., Bylaska E. J., 2004, Diversity of contaminant reduction reactions by zerovalent iron: role of the reductate, *Environ. Sci. Technol.*, 38, 139-147.
- 14) Zawaideh L. L., Zhang T. C., 1998, The effect of pH and addition of an organic buffer(HEPES) on nitrate transformation in Fe<sup>0</sup>-water systems, *Water Sci. Technol.*, 38, 107-115.
- 15) Cheremisinoff N. P., Cheremisinoff P. N., 1993, *Carbon adsorption for pollution control*, PTR Prentice Hall, 19pp.
- 16) Yang R. T., 조순행 역, 2006, 흡착제, 그 원리와 응용, 지구문화사, 149pp.
- 17) Arnold W. A., Roberts A. L., 2000, Pathways and kinetics of chlorinated ethylene and chlorinated acetylene reaction with Fe(0) particles, *Environ. Sci. Technol.*, 34, 1794-1805.
- 18) Till B. A., Weathers L. J., Alvarez P. J. J., 1998, Fe(0)-supported autotrophic denitrification, *Environ. Sci. Technol.*, 32, 634-639.
- 19) Froment G. F., Bischoff K. B., 1992, *Chemical reactor analysis and design*, 2nd ed., John Wiley & Sons, 90pp.